Published in final edited form as:
J Magn Reson Imaging. 2013 June ; 37(6): 1419–1426. doi:10.1002/jmri.23936.

Venous and Arterial Flow Quantification, are Equally Accurate and Precise with Parallel Imaging Compressed Sensing 4D Phase Contrast MRI

Umar Tariq, MBBS[1], **Albert Hsiao, MD, PhD**[1], **Marcus Alley, PhD**[1], **Tao Zhang, MS**[2], **Michael Lustig, PhD**[3], and **Shreyas S. Vasanawala, MD, PhD**[1]

[1]Department of Radiology, Stanford University, Stanford, CA USA

[2]Department of Electrical Engineering, Stanford University, Stanford, CA USA

[3]University of California Berkeley, Berkeley, CA USA

Abstract

Purpose—To evaluate precision and accuracy of parallel-imaging compressed-sensing 4D phase contrast (PICS-4DPC) MRI venous flow quantification in children with patients referred for cardiac MRI at our children's hospital.

Materials and Methods—With IRB approval and HIPAA compliance, 22 consecutive patients without shunts underwent 4DPC as part of clinical cardiac MRI examinations. Flow measurements were obtained in the superior and inferior vena cava, ascending and descending aorta and the pulmonary trunk. Conservation of flow to the upper, lower and whole body was used as an internal physiologic control. The arterial and venous flow rates at each location were compared with paired t-tests and F-tests to assess relative accuracy and precision.

RESULTS—Arterial and venous flow measurements were strongly correlated for the upper (ρ=0.89), lower (ρ=0.96) and whole body (ρ=0.97); net aortic and pulmonary trunk flow rates were also tightly correlated (ρ=0.97). There was no significant difference in the value or precision of arterial and venous flow measurements in upper, lower or whole body, though there was a trend toward improved precision with lower velocity-encoding settings.

Conclusion—With PICS-4DPC MRI, the accuracy and precision of venous flow quantification are comparable to that of arterial flow quantification at velocity-encodings appropriate for arterial vessels.

Keywords

Cardiovascular; 4D flow; flow quantification; compressed sensing; parallel imaging

Introduction

Blood flow quantification is an integral part of the diagnostic work-up for patients with congenital heart diseases (1). Two dimensional phase-contrast magnetic resonance imaging (2DPC MRI) is the most commonly employed and validated tool for evaluation of blood flow clinically (2–4). However it is a lengthy process requiring multiple predefined imaging planes and requiring direct physician oversight (5). In addition, flow quantification is limited to the vessels targeted during the scan (5). Several factors can influence the accuracy of flow

Address for Correspondence: Dr. Shreyas S Vasanawala, Department of Radiology, 725 Welch Road, Rm 1679 MC 5913, Stanford, CA 94305-5654, USA, TEL: 650-725-2548, FAX: 650-497-8745, vasanawala@stanford.edu.

quantification including the presence of complex flow (6) and eddy-current related phase offsets (7).

Volumetric, time-resolved phase contrast imaging (4DPC) (4,8,9) has potential for overcoming some of the limitations associated with 2DPC MRI (5), simultaneously measuring all three directional components of motion throughout an imaging volume (10,11). Since the entire volume is acquired simultaneously, this avoids the need to precisely define cross-sectional planes at the time of image acquisition. As opposed to 2DPC, there is no additional scan time required to evaluate other vessels in the imaging volume. Additionally with 2DPC, to measure blood flow in multiple vessels, multiple oblique plane scans have to be prescribed which may lead to spatial aliasing, causing abrupt phase discontinuities in the images. These phase discontinuities violate the assumptions of slowly varying background phase that underlie eddy current correction algorithms. However, with a volumetric data acquisition, spatial aliasing is easier to avoid, and thus eddy current correction can be more easily performed. Several groups have now shown potential advantages of 4DPC over 2DPC in characterizing pathological flow patterns in the heart, aorta, and brain (12–17). In addition, 4DPC has also been shown to have at least comparable quantitative accuracy and precision for arterial blood flow in the aorta and pulmonary trunk (18). More recently, arterial flow quantification has been shown to be more accurate and precise with 4DPC than 2DPC in congenital heart diseases (19).

The challenge of the lengthy scan time with 4DPC can be addressed by parallel imaging (PI) (20) and compressed sensing (CS) (21). PI can accelerate data acquisition by under-sampling k-space based on coil sensitivities. On the other hand, CS exploits image sparsity in some transform domain that makes under-sampling possible. Combining PI and CS (22), further data acquisition acceleration can be achieved. Previous study has shown that quantitative PICS-4DPC provides similar flow accuracy to 2DPC (23).

While the quantitative accuracy of 4DPC in large arterial vessels has been addressed, it is still unclear whether venous flow can be quantified with similar accuracy and precision at the velocity-encodings (vencs) that are required to avoid aliasing in the arterial vessels. This is of particular importance because multiple-vencs acquisitions are currently impractical to perform in the clinical environment due to time constraints. In theory, the velocity-to-noise ratio in these lower speed vessels should more adversely affect venous flow quantification (24). However, the significance of this effect has not been well evaluated in the clinical environment, especially in a pediatric patient population. We therefore sought to address whether accurate and precise venous flow measurements could be obtained from 4DPC in patients referred for cardiac MRI at our children’s hospital.

Materials and Methods

Patient Population

With institutional review board approval and HIPAA compliance, we retrospectively identified children referred for MRI at our hospital who underwent 4DPC acquisitions from March 2010 to July 2011. For the purposes of devising an internal control for flow quantification, patients with known shunts demonstrated either by echocardiography or MRI, were excluded. After reviewing patient charts, 22 consecutive patients (mean age 6 years, range 3–12 years) were identified. For a further sub-analysis, the population was then divided into two groups: 4DPC velocity-encoding speeds at or below 200 cm/s (n=12, age 6 +/− 5 years, range 2–12 years) and at or above 250 cm/s (n=10, age 8 +/− 7 years, range 3–14 years)(Table I).

Image Acquisition

All imaging was performed on a 1.5-T TwinSpeed MRI scanner (GE Healthcare, Milwaukee, WI) with 150 T/ms maximum slew rate, 40 mT/min gradients and vector ECG gating. The penultimate acquisition for each patient was an MRA with single dose gadofosveset. This was immediately followed by a 4D flow acquisition. 21 patients out of 22 patients in total were sedated for the MRI.

The 4-D flow data was acquired using an SPGR-based sequence with tetrahedral flow-encoding and 8-channel cardiac coil array. The following imaging parameters were used: frequency encoding direction L/R, flip angle 15°, average TE 1.8 ms, average TR 4.7 ms, average true temporal resolution of 53 ms, average FOV of 25 cm and 2–4 tetrahedral encodes per segment were used depending on heart rate. Average true temporal resolution was calculated as the product of views per segment and TR. Total number of uninterpolated slices ranged from 42 to 82. The matrix size was 256 × 192 in all the 4DPC acquisitions except in one, in which it was 256 × 224. K-space data was acquired with variable-density poisson disc undersampling with 2×2 to 2.2×2.2 reduction in two-phase encoding directions (25, 26). The total data acquisition reduction factor was between 4–5 and the actual scan time depending upon the heart rate and number of slices, ranged from 6 minutes 46 seconds to 14 minutes and 58 seconds with mean of 10 minutes and 44 seconds.

Respiratory compensation with k-space phase reordering (EXORCIST, GE Healthcare, Milwaukee, WI, USA) was employed without respiratory gating or navigation. 2DPC measurements were performed in all patients except two. Velocity-encoding (venc) parameters for 4DPC were selected to avoid aliasing using the lowest 2DPC venc that avoided aliasing. In the two patients without 2DPC measurements, the venc was chosen on the basis of clinical history. The first patient had coarctation of aorta and the venc was adjusted to 300 cm/sec; the second patient had a clinical suspicion of pulmonary sling so the venc was kept at 200 cm/sec. Images were reconstructed with L1-SPIRiT, a combined parallel-imaging and compressed sensing reconstruction algorithm (22, 27–30). 20 cardiac phases were retrospectively interpolated and distributed equally across the R-R interval. L1-SPIRiT was performed independently at each cardiac phase. Image data were volumetrically corrected for eddy-current-related phase offsets with a trilinear phase-offset model (18, 31). During the image reconstruction process, the data were corrected for Maxwell phase effects (32) and encoding errors due to gradient field distortions (33).

Flow Analysis

Flow quantification was performed with in-house developed software, as previously described (18). Slice planes were auto reformatted centered on the vessel lumen, oriented perpendicular to flow. Each vessel of interest was then manually segmented based on fused magnitude and velocity data. Calculations of net flow were computed with component of velocity perpendicular to the oblique plane. Three segmentations at adjacent levels were performed for each vessel. The mean of the three measurements was then used as an estimate of volumetric flow. Plane selection and segmentations were performed while blinded to any flow calculations.

Flow measurements were obtained in the superior vena cava, inferior vena cava, ascending aorta, descending aorta and pulmonary trunk (Figure 1). We defined upper body venous flow as the superior vena cava (SVC) flow; lower body venous flow as the inferior vena cava (IVC) flow and, whole body venous flow as the sum of superior vena cava flow and inferior vena cava flow (SVC+IVC). Similarly we defined upper body arterial flow as difference of blood flow in ascending aorta and descending aorta (AA-DA); lower body arterial flow as blood flow in descending aorta (DA) and whole body arterial flow as

ascending aorta flow (AA). To test the internal consistency of flow quantification, whole body venous flow was compared to whole body arterial flow and pulmonary trunk flow, upper body venous flow was compared to upper body arterial flow, and lower body venous flow was compared to lower body arterial flow.

Statistical Analysis

Statistical analyses were performed in Excel 2003 (Microsoft, Redmond, WA). The accuracy and precision of venous flow quantification was compared to arterial flow quantification in four ways. First, Pearson correlation coefficients between flow rates were calculated. Second, Bland-Altman analyses were performed to assess bias and limits of agreement. Third, paired t-tests were used to identify systematic differences in the flow rates. Fourth, in order to assess the precision of venous flow measurements relative to arterial flow measurements, we compared the aortopulmonary error with the arteriovenous error. The aortopulmonary error was defined as the difference between aortic and pulmonary flow rates for each patient. The arteriovenous errors were defined as the differences between arterial and venous flow rates for each the upper, lower and whole body. F-tests were then used to compare the aortopulmonary and arteriovenous errors. This analysis was used as a benchmark to assess precision of venous flow measurements. A type I error rate of 0.05 was used for all statistical tests.

Results

Table II summarizes the correlation and the extent of agreement between flow measurements among the arterial and venous vessels. Bland-Altman plots are shown in Figure 2.

Accuracy

Upper body venous and arterial flow rates were well correlated (ρ=0.89) with venous flows exceeding arterial flows by 6%, on average. This difference was not statistically significant ($p>0.05$, paired t-test). Similarly, lower body venous and arterial flow rates were also well correlated (ρ=0.96) with arterial flows exceeding venous flows by 6%, on average. Again, this difference was not statistically significant ($p>0.05$, paired t-test).

Whole body venous flow rates were tightly correlated with both pulmonary trunk flow rates (ρ=0.94) and whole body arterial flow rates (ρ=0.97). Pulmonary trunk flow rates slightly exceeded whole body venous flow rates by 2%, which was not significant ($p>0.05$, paired t-test). However, whole body arterial flow rates exceeded whole body venous flow rates by 7%. This finding was statistically significant ($p<0.05$, paired t-test). As expected, whole body arterial flow rates also exceeded pulmonary trunk flow rates by 4% though this did not reach statistical significance ($p>0.05$, paired t-test). These results are consistent with that of a previous study comparing aortic and pulmonary flow, where observed mean difference was 3–4% of flow rate (18, 34). The arteriovenous difference for upper body (0.1 L/min), lower body (0.1 L/min) and whole body (0.2 L/min) were comparable to aortopulmonary difference (0.1 L/min). However there was increased arteriovenous relative difference for upper body (6%), lower body (6%) and whole body (7%) compared to aortopulmonary relative difference (4%). The decreased amount of flow in the upper and lower body as compared to whole body explains the increased arteriovenous relative differences. Moreover this did not reach statistical significance ($p>0.05$, paired t-test).

To determine if the location of measurements affected the accuracy of flow rates, we also measured flow in descending thoracic aorta in two locations: just distal to the last arch

vessel and proximal to the diaphragmatic hiatus. These flow rates were also tightly correlated (ρ=0.98) with no significant difference in the flow rates ($p<0.05$, paired t-test).

Precision

Upper body venous and arterial flows were well matched with Bland-Altman limits of agreement from −0.5 L/min to 0.3 L/min. Lower body venous and arterial flows were also well matched with Bland-Altman limits of agreement from −0.3 L/min to 0.4 L/min. Similarly, whole body venous and arterial flows were also well matched with Bland-Altman limits of agreement from −0.3 L/min to 0.6 L/min. Additionally, whole body arterial and pulmonary trunk flows were well matched with Bland-Altman limits of agreement from −0.6 L/min to 0.4 L/min, and these limits of agreement are each in line with prior studies comparing aortic and pulmonary flow rates (18, 34).

The arteriovenous limits of agreement for upper body (−0.5 L/min to 0.3 L/min), lower body (−0.3 L/min to 0.4 L/min) and whole body (−0.3 L/min to 0.6 L/min) were comparable to aortopulmonary limits of agreement (−0.6 L/min to 0.4 L/min); however arteriovenous relative limits of agreement for upper body (−44% to 32%) and lower body (−22% to 34%) were wider than aortopulmonary relative limits of agreement (−22% to 14%) due to decreased flow in upper and lower body. Whole body arteriovenous relative limits of agreement (−13% to 26%) were comparable to aortopulmonary relative limits of agreement (−22% to 14%). We performed a further analysis to determine whether the venous flow measurements had a greater degree of error by comparing aortopulmonary and arteriovenous errors. No statistically significant differences could be found for the upper body (F-test p=0.47), lower body (F-test p=0.31) or whole body (F-test p=0.92).

Pulmonary regurgitation in the post-operative tetralogy of fallot patients is known to potentially result in inaccuracies of pulmonary blood flow quantification, which can result in increased difference of flow in our aorto-pulmonary pair. To address this potential pitfall, we did a stratified analysis comparing our sub-population of post-operative tetralogy of fallot subject versus the remaining population subjects; no significant change was found in this difference of aorto-pulmonary flow (p=0.24, unpaired t-test and p=0.22, F-test).

In coarctation of aorta patients, there may be a collateral flow via the internal mammary or intercostal arteries, which might lead to variation of descending aorta flow measurements along its length. However in our sub-population of coarctation of aorta patients, there was no significant increase in the difference of flow between the descending aorta after last arch vessel and the descending aorta just before diaphragm (p=0.97, unpaired t-test & p=0.12, F-test) as compared to the remaining population.

Stratified Analysis

Finally, to determine whether velocity-encodings (vencs) affected the precision of our quantitative flow measurements, we performed a stratified analysis of measurements obtained at higher vencs (at or above 250 cm/s) and lower vencs (at or below 200 cm/s). While comparing our higher and lower venc groups, both groups had comparable age (lower venc group n=12, age 6 +/− 5 years, range 2–12 years and higher venc group n=10, age 8 +/− 7 years, range 3–14 years) with no statistically significant difference (p=0.16, unpaired t-test & p=0.47, F-test). Table III summarizes the results at higher and lower vencs. In this analysis, we observed slight differences in the upper body flow measurements at lower and higher vencs. There appeared to be greater variation between the arterial and venous flows with higher vencs (Bland Altman limits ranging from −0.6 L/min to 0.3 L/min vs −0.3 L/min to 0.2 L/min) as shown in Figure 3. This finding tended to but it did not reach statistical significance (p=0.08, F-test). Arterial and venous flow measurements at lower vencs were

also more tightly correlated ($\rho=0.96$ *vs* $\rho=0.88$) in upper body. However, in lower body flow measurements at lower and higher vencs, there was not much difference and it did not reach statistical significance (p=−0.21, F-test). Similarly, in whole body flow measurements at lower and higher vencs, again there was not much difference and it also did not reach statistical significance (p=0.27, F-test).

Discussion

Our study demonstrates that with 4DPC MRI, the accuracy and precision of venous flow quantification are comparable to that of arterial flow quantification in children undergoing MRI for cardiovascular disease. While acquiring flow data, the vencs value is adjusted to the highest velocity within the chosen 4D volume to prevent aliasing; this might lead to increased error and inaccuracy for blood flow quantification in low-velocity vessels (24). We showed venous flow measurements can be obtained with reasonable accuracy, at vencs appropriate for arterial vessels. However, our results suggest lower vencs settings further improve venous flow assessment, though one must weigh whether the potential added precision is worth the cost of additional imaging time, for a separate low vencs acquisition. In such a case, the venc settings should be chosen depending upon a spectrum of parameters including patients' age, clinical history, velocity of flow and the availability of anti-aliasing software.

Quantitative flow measurement is an important part of cardiovascular MRI studies in patients with congenital heart disease (35–37). So far, the validation studies of 4D flow have focused mainly on arterial flow (18, 34, 38–39). One major indication of using MRI in congenital heart disease is to quantify blood flow. Historically, this has been primarily for arterial flow. However, venous flow assessment may be of value in patients who on a single ventricle pathway e.g. Glenn or Fontan subjects. Additionally, we are seeing subjects in whom pulmonary venous flow quantification may be helpful. 4D flow provides many advantages including saving time by avoiding repeat planning and acquisition of imaging planes, perpendicular to multiple vessel of interest; thus data analysis is not limited to the acquired predefined 2D imaging plane. Moreover 4D has further potential advantage of measuring blood flow patterns not otherwise apparent on 2D.

There are two particular sub-segments of circulation that may have an impact on our flow measurements. One is the coronary flow, which passes through in sequence through *aorta*, coronary arteries, coronary veins, right atrium, right ventricle, *pulmonary artery* and pulmonary veins, but never contributing to caval flow. The other is bronchial circulation, the majority of which drains from bronchial arteries to pulmonary veins rather than bronchial veins (40). Thus bronchial flow passes through the *aorta*, but not cavae nor pulmonary artery. Combining the effects of these two sub-segments of circulation, we would expect the pulmonic flows to exceed caval flow by the coronary flow volume and the aortic flow to exceed the pulmonic flow by the bronchial flow volume. In our population, we in fact found pulmonic flow exceeding caval flow by 2% and aortic flow exceeding pulmonic flow by 4%.

There are some limitations associated with our study. First, we did not perform a direct evaluation of accuracy and precision of 4DPC venous flow quantification as compared to the 2DPC venous flow quantification. We performed an indirect assessment of accuracy and precision of 4DPC venous flow quantification. As the greater consistency of 4DPC for arterial flow quantification over 2DPC has already been established, we compared the consistency of flow measurements of the aorto-pulmonary pair (with both arterial components) with consistency of the of flow measurements of the arterio-venous pairs to evaluate if they both had comparable consistency, thus indirectly assessing the accuracy of

venous flow measurements. Second, this is a single-center study in a group of patients with congenital heart diseases. Additional research is needed to further validate the accuracy of 4D blood flow measurements in a larger group of patients in a multi-center approach. Moreover the acquisition parameters are not uniform across all patients; in a clinical setting, MRI exams are tailored to each patient to account for the clinical needs, patient size, heart rate and available acquisition time but this represents a spectrum typical of modern practice.

In conclusion, this work shows the accuracy and precision of venous flow quantification with 4D flow are comparable to that of arterial flow quantification in children undergoing cardiac MRI for cardiovascular disease.

Acknowledgments

The authors are grateful for the support of the John and Tashia Morgridge Foundation, the National Institutes of Health (grant R01 EB009690 to S. S. Vasanawala), American Heart Association Grant #12BGIA9660006, UC Discovery #193037, GE Healthcare, and NVIDIA.

References

1. Beerbaum P, Korperich H, Barth P, Esdorn H, Gieseke J, Meyer H. Noninvasive quantification of left-to-right shunt in pediatric patients: phase-contrast cine magnetic resonance imaging compared with invasive oximetry. Circulation. 2001; 103:2476–2482. [PubMed: 11369688]
2. Szolar DH, Sakuma H, Higgins CB. Cardiovascular applications of magnetic resonance flow and velocity measurements. J Magn Reson Imaging. 1996; 6:78–89. [PubMed: 8851410]
3. Higgins CB, Sakuma H. Heart disease: functional evaluation with MR imaging. Radiology. 1996; 199:307–315. [PubMed: 8668769]
4. Pelc NJ, Herfkens RJ, Shimakawa A, Enzmann DR. Phase contrast cine magnetic resonance imaging. Magn Reson Q. 1991; 7:229–254. [PubMed: 1790111]
5. Nordmeyer S, Riesenkampff E, Crelier G, et al. Flow-sensitive four-dimensional cine magnetic resonance imaging for offline blood flow quantification in multiple vessels: a validation study. J Magn Reson Imaging. 2010; 32:677–683. [PubMed: 20815066]
6. Kilner PJ, Henein MY, Gibson DG. Our tortuous heart in dynamic mode--an echocardiographic study of mitral flow and movement in exercising subjects. Heart Vessels. 1997; 12:103–110. [PubMed: 9496460]
7. Gatehouse PD, Rolf MP, Graves MJ, et al. Flow measurement by cardiovascular magnetic resonance: a multi-centre multi-vendor study of background phase offset errors that can compromise the accuracy of derived regurgitant or shunt flow measurements. J Cardiovasc Magn Reson. 2010; 12:5. [PubMed: 20074359]
8. Alley MT, Napel S, Amano Y, et al. Fast 3D cardiac cine MR imaging. J Magn Reson Imaging. 1999; 9:751–755. [PubMed: 10331775]
9. Pelc NJ, Bernstein MA, Shimakawa A, Glover GH. Encoding strategies for three-direction phase-contrast MR imaging of flow. J Magn Reson Imaging. 1991; 1:405–413. [PubMed: 1790362]
10. Wigstrom L, Sjoqvist L, Wranne B. Temporally resolved 3D phase-contrast imaging. Magn Reson Med. 1996; 36:800–803. [PubMed: 8916033]
11. Markl M, Kilner PJ, Ebbers T. Comprehensive 4D velocity mapping of the heart and great vessels by cardiovascular magnetic resonance. J Cardiovasc Magn Reson. 2011; 13:7. [PubMed: 21235751]
12. Hope MD, Hope TA, Crook SE, et al. 4D flow CMR in assessment of valve-related ascending aortic disease. JACC Cardiovasc Imaging. 2011; 4:781–787. [PubMed: 21757170]
13. Markl M, Draney MT, Hope MD, et al. Time-resolved 3-dimensional velocity mapping in the thoracic aorta: visualization of 3-directional blood flow patterns in healthy volunteers and patients. J Comput Assist Tomogr. 2004; 28:459–468. [PubMed: 15232376]

14. Hope TA, Markl M, Wigstrom L, Alley MT, Miller DC, Herfkens RJ. Comparison of flow patterns in ascending aortic aneurysms and volunteers using four-dimensional magnetic resonance velocity mapping. J Magn Reson Imaging. 2007; 26:1471–1479. [PubMed: 17968892]
15. Isoda H, Ohkura Y, Kosugi T, et al. In vivo hemodynamic analysis of intracranial aneurysms obtained by magnetic resonance fluid dynamics (MRFD) based on time-resolved three-dimensional phase-contrast MRI. Neuroradiology. 2010; 52:921–928. [PubMed: 20012431]
16. van der Hulst AE, Westenberg JJ, Kroft LJ, et al. Tetralogy of fallot: 3D velocity-encoded MR imaging for evaluation of right ventricular valve flow and diastolic function in patients after correction. Radiology. 2010; 256:724–734. [PubMed: 20634432]
17. Geiger J, Markl M, Jung B, et al. 4D-MR flow analysis in patients after repair for tetralogy of Fallot. Eur Radiol. 2011; 21:1651–1657. [PubMed: 21720942]
18. Hsiao A, Alley MT, Massaband P, Herfkens RJ, Chan FP, Vasanawala SS. Improved cardiovascular flow quantification with time-resolved volumetric phase-contrast MRI. Pediatr Radiol. 2011; 41:711–720.2. [PubMed: 21221566]
19. Hsiao A, Lustig M, Alley MT, et al. Rapid pediatric cardiac assessment of flow and ventricular volume with compressed sensing parallel imaging volumetric cine phase-contrast MRI. AJR Am J Roentgenol. 2012; 198:W250–9. [PubMed: 22358022]
20. Griswold M, Jakob P, Heidemann R, Nittka M, Jellus V, Wang J, Kiefer B, Haase A. Generalized autocalibrating partially parallel acquisitions (GRAPPA). Magn Reson Med. 2002; 47:1202–1210. [PubMed: 12111967]
21. Lustig M, Donoho D, Pauly J. Sparse MRI: The application of compressed sensing for rapid MR imaging. Magn Reson Med. 2007; 58:1182–1195. [PubMed: 17969013]
22. Lustig M, Pauly JM. SPIRiT: Iterative self-consistent parallel imaging reconstruction from arbitrary k-space. Magn Reson Med. 2010; 64:457–471. [PubMed: 20665790]
23. Hsiao, A.; Lustig, M.; Alley, MT.; Murphy, M.; Vasanawala, SS. Quantitative assessment of blood flow with 4D phase-contrast MRI and autocalibrating parallel imaging compressed sensing. Proceedings of the 19thAnnual Meeting of ISMRM; Montreal. 2011. p. 1190
24. Pelc NJ, Sommer FG, Li KC, Brosnan TJ, Herfkens RJ, Enzmann DR. Quantitative magnetic resonance flow imaging. Magn Reson Q. 1994; 10:125–147. [PubMed: 7811608]
25. Markl M, Chan FP, Alley MT, et al. Time-resolved three-dimensional phase-contrast MRI. J Magn Reson Imaging. 2003; 17:499–506. [PubMed: 12655592]
26. Bammer R, Hope TA, Aksoy M, Alley MT. Time-resolved 3D quantitative flow MRI of the major intracranial vessels: initial experience and comparative evaluation at 1.5T and 3. 0T in combination with parallel imaging. 2007; 57:127–140.
27. Vasanawala SS, Alley MT, Hargreaves BA, Barth RA, Pauly JM, Lustig M. Improved pediatric MR imaging with compressed sensing. Radiology. 2010; 256:607–616. [PubMed: 20529991]
28. Vasanawala SS, Lustig M. Advances in pediatric body MRI. Pediatr Radiol. 2011; 41 (Suppl 2): 549–554. [PubMed: 21847737]
29. Murphy M, Alley M, Demmel J, Keutzer K, Vasanawala S, Lustig M. Fast ℓ_1-SPIRiT Compressed Sensing Parallel Imaging MRI: Scalable Parallel Implementation and Clinically Feasible Runtime. IEEE Trans Med Imaging. 201210.1109/TMI.2012.2188039
30. Hsiao, A.; Alley, MT.; Murphy, MJ.; Lustig, M.; Vasanawala, SS. Quantitative Assessment of blood Flow with 4D Phase-Contrast MRI and Autocalibrating Parallel Imaging Compressed Sensing. Proceedings of the 11th Annual Meeting of ISMRM; Montreal, Canada. 2000. (Poster 1190)
31. Walker PG, Cranney GB, Scheidegger MB, Waseleski G, Pohost GM, Yoganathan AP. Semiautomated method for noise reduction and background phase error correction in MR phase velocity data. J Magn Reson Imaging. 1993; 3:521–530. [PubMed: 8324312]
32. Bernstein MA, Zhou XJ, Polzin JA, et al. Concomitant gradient terms in phase contrast MR: analysis and correction. Magn Reson Med. 1998; 39:300–8. [PubMed: 9469714]
33. Markl M, Bammer R, Alley MT, et al. Generalized reconstruction of phase contrast MRI: analysis and correction of the effect of gradient field distortions. Magn Reson Med. 2003; 50:791–801. [PubMed: 14523966]

34. Brix L, Ringgaard S, Rasmusson A, Sorensen TS, Kim WY. Three dimensional three component whole heart cardiovascular magnetic resonance velocity mapping: comparison of flow measurements from 3D and 2D acquisitions. J Cardiovasc Magn Reson. 2009; 11:3. [PubMed: 19232119]

35. Kilner PJ, Geva T, Kaemmerer H, Trindade PT, Schwitter J, Webb GD. Recommendations for cardiovascular magnetic resonance in adults with congenital heart disease from the respective working groups of the European Society of Cardiology. Eur Heart J. 2010; 31:794–805. [PubMed: 20067914]

36. Powell AJ, Geva T. Blood flow measurement by magnetic resonance imaging in congenital heart disease. Pediatr Cardiol. 2000; 21:47–58. [PubMed: 10672614]

37. Powell AJ, Maier SE, Chung T, Geva T. Phase-velocity cine magnetic resonance imaging measurement of pulsatile blood flow in children and young adults: in vitro and in vivo validation. Pediatr Cardiol. 2000; 21:104–110. [PubMed: 10754076]

38. Uribe S, Beerbaum P, Sorensen TS, Rasmusson A, Razavi R, Schaeffter T. Four-dimensional (4D) flow of the whole heart and great vessels using real-time respiratory self-gating. Magn Reson Med. 2009; 62:984–992. [PubMed: 19672940]

39. Sorensen TS, Beerbaum P, Korperich H, Pedersen EM. Three-dimensional, isotropic MRI: a unified approach to quantification and visualization in congenital heart disease. Int J Cardiovasc Imaging. 2005; 21:283–292. [PubMed: 16015442]

40. Charan NB, Thompson WH, Carvalho P. Functional anatomy of bronchial veins. Pulm Pharmacol Ther. 2007; 20:100–103. [PubMed: 16807022]

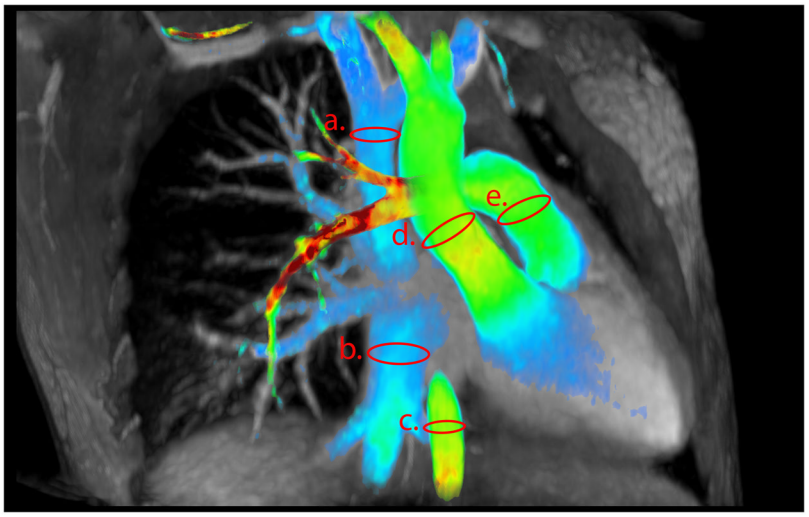

Figure 1.

(a) Superior vena cava, (b) inferior vena cava, (c) descending aorta, (d) ascending aorta and (e) pulmonary trunk flow rates were measured. The precision of flow utilizing a vein & an artery was then determined. This was done in pairs for the upper body (superior vena cava flow vs difference between ascending and descending aortic flow), lower body (inferior vena cava flow vs descending aortic flow) and whole body (sum of superior vena cava and inferior vena cava flow vs ascending aortic flow).

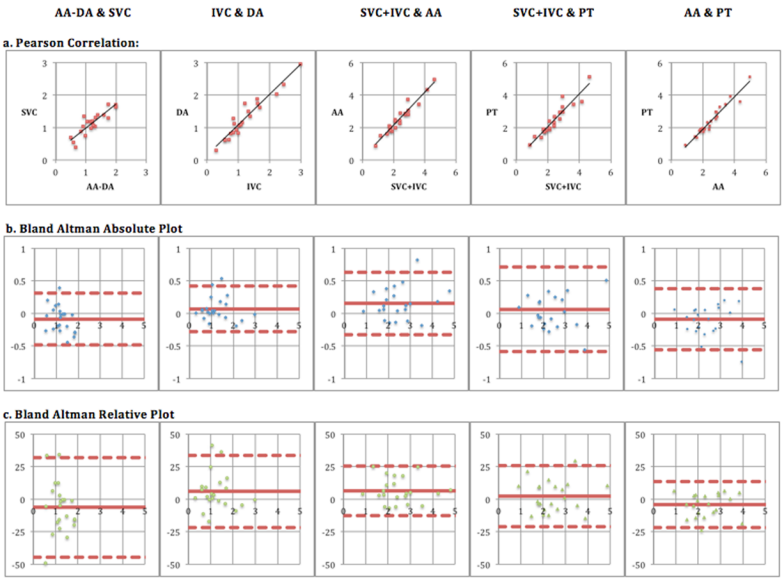

Figure 2.

(a) Correlation, (b) Bland Altman Absolute comparison & (c) Bland Altman Relative/ Percent Difference comparison of Arterial & Venous Flow Quantification by 4-D phase contrast MRI (x-axis represent mean and y-axis represent difference (units: L/min in absolute plot & relative percentage in relative plot)). The outer dashed lines indicate the limits of agreement. Lower limit of agreement represents the mean difference −1.96 standard deviations and upper limit of agreement represents the mean difference +1.96 standard deviations. AA= Ascending Aorta, DA= Descending Aorta after last arch vessel, PT= Pulmonary Trunk, SVC= Superior Vena Cava, IVC= Inferior Vena Cava

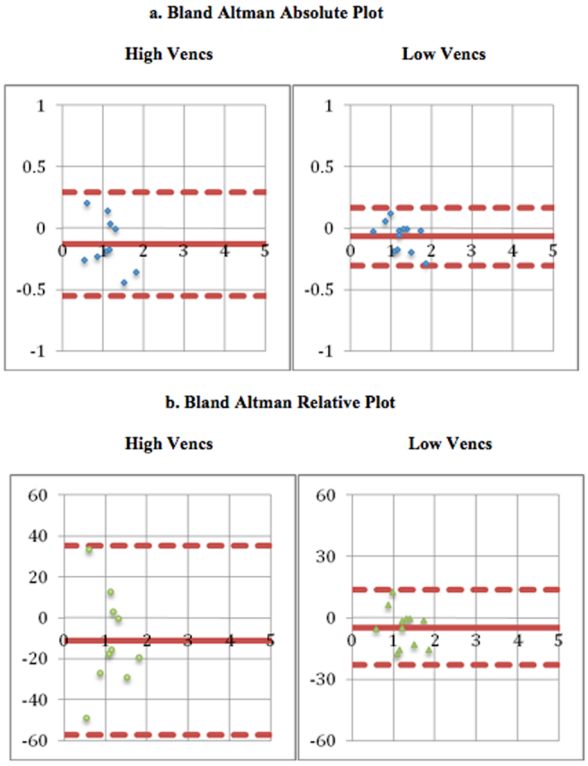

Figure 3.

(a) Bland Altman Absolute comparison & (b) Bland Altman Relative/Percent Difference of high vencs (250 or above) population (n=10) and low vencs (200 & below) population (n=12) for arterial & venous flow quantification in upper body (x-axis represent mean and y-axis represent difference (units: L/min in absolute plot & relative percentage in relative plot)). The outer dashed lines indicate the limits of agreement. Lower limit of agreement represents the mean difference −1.96 standard deviations and upper limit of agreement represents the mean difference +1.96 standard deviations.

J Magn Reson Imaging. Author manuscript; available in PMC 2014 June 01.

Table I

The age, weights, body surface area and clinical history of all patients are listed. The velocity-encoding (vencs) parameter is also shown

Pt No.	Age(Y)	Weight (kg)	Body Surface Area(m2)	Venc s(cm/s)	Clinical History
1	7	26.9	0.97	300	Truncus Arteriousus, post-repair
2	3	15	0.68	150	ToF, post-repair
3	7	23	0.89	200	Pulmonary Hypertension
4	8	20.1	0.81	250	ToF, post-repair
5	8	29	1.04	150	Post liver transplant
6	10	10.3	0.46	300	Coarctation of Aorta
7	14	59	1.66	250	Interrupted Aortic Arch, post-repair
8	7	23	0.89	200	ToF, post-repair
9	3	15	0.69	200	Respiratory Impairment
10	5	4.8	0.25	200	Bicuspid Aortic Valve
11	3	12	0.53	250	ToF, post-repair
12	6	36	1.1	350	ToF, post-repair
13	5	16	0.69	200	Ebstein's Anomaly & Pulmonary Insufficiency
14	4	17	0.68	200	TGA-post repair
15	6	26	0.95	250	TGA-post repair
16	6	20	0.78	200	Abnormal Tricuspid valve
17	7	25	0.96	200	Coarctation of Aorta, post-repair
18	9	20.9	0.84	300	Double Outlet right ventricle
19	12	56	1.37	200	Coarctation of Aorta, post-repair
20	2	12	0.5	180	Coarctation of Aorta, post-repair
21	6	25	0.95	250	ToF, post-repair
22	4	17	0.69	300	Coarctation of Aorta

ToF= Tetralogy of Fallot, TGA= Transposition of Great Arteries

Table II

Statistical Comparison of Various Flows by 4-D phase contrast (n=22). Lower limit of agreement represents the mean difference −1.96 standard deviations and upper limit of agreement represents the mean difference +1.96 standard deviations

	Upper Body	Lower Body	Whole Body	Whole Body	Whole Body	Lower Body
Flow A	**AA- DA**	**IVC**	**SVC + IVC**	**SVC + IVC**	**AA**	**DAD**
Flow B	**SVC**	**DA**	**AA**	**PT**	**PT**	**DA**
Pearson Correlation Coefficient	0.89	0.96	0.97	0.94	0.97	0.98
Paired T-test p values	0.06	0.09	0.01	0.38	0.89	0.72
Bland-Altman Absolute						
Mean Difference (L/min)	−0.1	0.1	0.2	0.1	−0.1	0
Lower Limit of Agreement (L/min)	−0.5	−0.3	−0.3	−0.6	−0.6	−0.2
Upper Limit of Agreement (L/min)	0.3	0.4	0.6	0.7	0.4	0.3
Bland-Altman Relative						
Mean Difference	−6%	6%	7%	2%	−4%	1%
Lower Limit of Agreement	−44%	−22%	−13%	−21%	−22%	−18%
Upper Limit of Agreement	32%	34%	26%	26%	14%	21%

AA= Ascending Aorta, DA= Descending Aorta after last arch vessel, DAD= Descending Aorta just above diaphragm, PT= Pulmonary Trunk, SVC= Superior Vena Cava, IVC= Inferior Vena Cava

Table III

Statistical Comparison of high vencs (250 or above) population (n=10) and low vencs (200 & below) population (n=12) for arterial & venous flow measurements in upper, lower & whole body. Lower limit of agreement represents the mean difference −1.96 standard deviations and upper limit of agreement represents the mean difference +1.96 standard deviations

	Upper Body		Lower Body		Whole Body	
Flow A	**AA-DA**		**IVC**		**SVC+IVC**	
Flow B	**SVC**		**DA**		**AA**	
	High vencs	**Low vencs**	**High vencs**	**Low vencs**	**High vencs**	**Low vencs**
Pearson Correlation Coefficient	0.88	0.96	0.99	0.97	0.98	0.99
BLAND - ALTMAN ABSOLUTE						
Mean Difference (L/min)	−0.1	−0.1	0.1	0	0.2	0.1
Lower Limit of Agreement (L/min)	−0.6	−0.3	−0.2	−0.3	−0.2	−0.2
Upper Limit of Agreement (L/min)	0.3	0.2	0.3	0.3	0.6	0.4
BLAND - ALTMAN RELATIVE						
Mean Difference	11%	−5%	5%	3%	8%	4%
Lower Limit of Agreement	−57%	−23%	−15%	−25%	−13%	9%
Upper Limit of Agreement	35%	14%	24%	31%	29%	18%

AA= Ascending Aorta, DA= Descending Aorta, SVC= Superior Vena Cava, IVC= Inferior Vena Cava